

# Synaptic shunting by a baseline of synaptic conductances modulates responses to inhibitory input volleys in cerebellar Purkinje cells

Lisa Kreiner and Dieter Jaeger

Department of Biology, Emory University, Atlanta GA, USA

When processing synaptic input *in vivo*, large neurons in the brain must cope with thousands of events each second. Much work has focused on the specific processing of synchronous excitatory input volleys, both in cerebellar and cerebral cortical research. Here we pursue the question of how a continuous background of ongoing 'noise' inputs interacts with the processing of synchronous inhibitory input volleys. Specifically we examine the processing of inhibitory input transients in cerebellar Purkinje cells, which by inducing pauses in Purkinje cell spike activity may lead to a disinhibition of the deep cerebellar nuclei and thus to cerebellar motor command signals. We use the technique of dynamic clamping *in vitro* to simulate controlled patterns of *in vivo* like background inputs. We use electrical stimulation of inhibitory interneurons in the deep or upper molecular layer to create inhibitory input transients that lead to spike pauses in Purkinje cell activity. These pauses were much longer in the absence than in the presence of background inputs applied with dynamic clamping. We found that a significant amount of the synaptic current elicited by electrical stimulation was shunted by the background inputs. The overall amount of background conductance as well as the pattern of background inputs modulated spike pause duration in a specific manner. This modulation by shunting may be employed *in vivo* to evaluate the salience of specific sensory input received by cerebellar cortex.

## Keywords:

**synaptic coding - spike timing - cerebellum - shunting - dynamic clamp - inhibition**

Kreiner L, Jaeger D.

Synaptic shunting by a baseline of synaptic conductances modulates responses to inhibitory input volleys in cerebellar Purkinje cells  
*Cerebellum* 2004; 3: 112-125

## Introduction

*In vivo*, neurons do not process synaptic inputs in isolation, but in the context of ongoing background activity. The amount of background activity likely to occur has a strong influence on synaptic integration by dramatically changing the input resistance and time constant of neurons.<sup>1,2</sup> These changes lead to a significant shunting of membrane currents, as well as a faster response time. It has been shown that inhibitory inputs shunt spike responses *in vivo*, for example thalamic bursting<sup>3</sup> and cortical visual responses<sup>4</sup> can be shunted. In principle, however, the amount of shunting is proportional to the total amount of excitatory and inhibitory conductance, and in the case of an ongoing background of excitation and inhibition, shunting is expected to have a strong effect on synaptic integration.<sup>5,6</sup> In addition, noise fluctuations in the input conductance have important influences on the properties of the output spike

train<sup>7,8</sup> as well as the interaction between inhibitory and excitatory inputs.<sup>9</sup>

Purkinje cells in the cerebellar cortex are likely to receive a large amount of background excitation from parallel fiber inputs and inhibition from interneurons that are also activated by parallel fibers. Such input results in an irregular firing pattern, in which spike timing is mostly controlled by inhibition and intrinsic currents.<sup>5,10</sup> Superimposed on this background synaptic activity, synchronized input volleys are likely to occur as a result of activation of specific populations of granule cells during behavior.<sup>11</sup> These volleys could specifically affect Purkinje cells overlying activated granule cell populations via synaptic output on the ascending branch of granule cell axons,<sup>12</sup> or via synchronized parallel fiber activity. In either case, such granule cell activation is expected to lead to synchronized excitatory as well as inhibitory inputs onto specific populations of Purkinje cells. Since the output of Purkinje cells is inhibitory onto the deep cerebellar nuclei, spike pauses in Purkinje cell activity are likely the relevant signal by which motor commands are transmitted to the deep cerebellar nuclei.<sup>6,13,14</sup>

In the present study we examine the hypothesis that the level of background input a Purkinje cell receives selectively shapes the response to inhibitory input volleys by the mechanism of synaptic shunting. We hypothesize that the overall level of parallel fiber activity may have a strong effect on the expression of behaviorally relevant spike pauses. We use the technique of dynamic clamp-

Received 8 October 2003; Revised 16 February 2004; Accepted 8 March 2004

## Correspondence:

Dieter Jaeger, Department of Biology, Emory University, 1510 Clifton Road, Atlanta, GA, 30322 USA.

Tel: +1 404 727 8139. Fax: +1 404 727 2880.

E-mail: [djaeger@emory.edu](mailto:djaeger@emory.edu)

© 2004 Taylor & Francis

DOI 10.1080/14734220410031990

ing<sup>15,16</sup> to apply a controlled pattern of background conductances to Purkinje cells recorded in rat brain slices while using electrical stimulation of interneurons to elicit inhibitory synaptic responses. We find that synaptic shunting indeed significantly shapes the response to brief bursts of inhibitory input. Thus synaptic shunting provides a mechanism by which parallel fiber activity sets the context under which synchronized volleys of input are processed.<sup>12</sup> Cerebellar cortical processing may thus occur via the interaction of an asynchronous continuous input mode and a synchronous mode of specific input volleys.

## Materials and methods

### Slice preparation and whole cell recording

All animal procedures fully complied with the National Institutes of Health guidelines on animal care and use and were conducted under a protocol approved by the Emory IACUC. Sprague-Dawley rats (15–21 days old) were anesthetized with halothane, decapitated, and the brain was quickly removed and dropped into ice-cold oxygenated Ringer. Slices were cut in the sagittal plane with a 300  $\mu\text{M}$  thickness and incubated following standard procedures.<sup>6</sup> Whole-cell recordings were obtained from the soma of visualized Purkinje cells at 32 °C using an extracellular medium containing (in mM): 124 NaCl, 3 KCl, 1.9 MgSO<sub>4</sub>, 1.2 KH<sub>2</sub>PO<sub>4</sub>, 26 NaHCO<sub>3</sub>, 2 CaCl<sub>2</sub>, and 20 Glucose, and oxygenated with 95% O<sub>2</sub> and 5% CO<sub>2</sub>. Electrodes were filled with (in mM): 140 Potassium Gluconate, 10 HEPES, 6 NaCl, 2 MgCl<sub>2</sub>, 0.2 EGTA, 4 NaATP, 0.4 NaGTP, 0.05 Spermine, and 5 Glutathione. This solution was adjusted to a pH of 7.3 with KOH, and slightly diluted to 270 mOsm with distilled water. The computed Cl<sup>-</sup> reversal potential given the final chloride concentrations in the extracellular and intracellular media is -70 mV. Electrodes had an impedance between 5 and 10 M $\Omega$ . Electrode tips were coated with Sylgard, which provided a significant reduction in capacitive artifacts during dynamic clamping. Endogenous excitatory input in the slices via AMPA receptors was blocked with 30  $\mu\text{M}$  CNQX in the extracellular solution. NMDA receptors were blocked with 100  $\mu\text{M}$  AP-5 and metabotropic glutamate receptors (mGluRs) were blocked with either 500  $\mu\text{M}$  MCPG or a mixture of 50  $\mu\text{M}$  LY367385, 0.5  $\mu\text{M}$  CPPG and 0.5  $\mu\text{M}$  MPEP hydrochloride. All pharmacological blockers were purchased from Tocris Cookson (St. Louis, MO).

### Electrical stimulation

Basket and stellate cells in the molecular layer of the cerebellum were electrically stimulated with a pipette filled with 0.5 M NaCl. These stimulating pipettes were similar in size and tip diameter to whole-cell recording electrodes; thus stimulating only a small local patch of tissue.<sup>17</sup> To avoid stimulating cells that present a

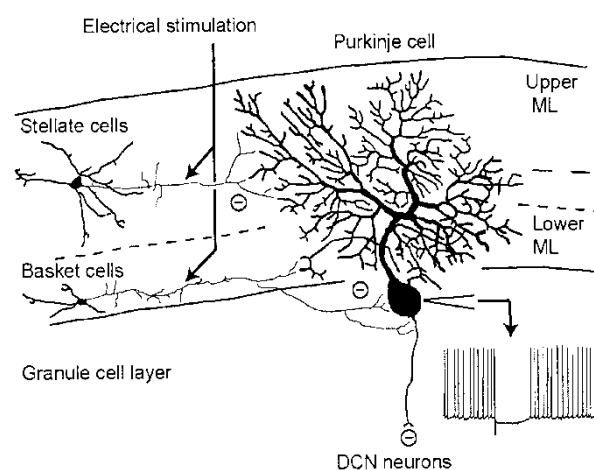


**Figure 1**

Schematic drawing of electrical stimulation in the molecular layer. Electrical stimulation was applied to either the lower or upper third of the molecular layer in order to stimulate presumed basket or stellate cells, respectively. Stimulating either type of interneuron could elicit a pause in Purkinje cell spiking (voltage trace). Purkinje cells are the only output neurons of the cerebellar cortex and make inhibitory synaptic connections onto deep cerebellar nuclei (DCN) neurons.

transition between true basket and stellate cell types at an intermediate depth in the molecular layer,<sup>18</sup> we used stimulation sites only in the lower- or uppermost 1/3rd of the molecular layer (Fig. 1). Axons of interneurons primarily remain at the depth of the cell soma in the molecular layer,<sup>19</sup> and thus favor a cell-type specific stimulation of interneurons at different depths. However, some branches of basket cell axons ascend into the upper molecular layer and could lead to a component of basket cell stimulation even for superficial stimulation sites. Biphasic stimulation pulses of 0.2 ms biphasic pulse were given through a stimulus isolator (World Precision Instruments, model A365). Stimulation strength was increased until a pause response was seen in spontaneous Purkinje cell spiking. Required stimulation intensities ranged from 8–80 V (measured on an oscilloscope in parallel to the stimulation electrode). This is equivalent to stimulation currents of 1.6–16  $\mu\text{A}$  for an electrode impedance of 5 Meg $\Omega$ , which is a typical value for the patch electrodes used. Due to the presence of blockers of all excitatory synaptic transmission, the direct stimulation of parallel fibers did not lead to any responses.

### Dynamic current clamp

In order to simulate the background synaptic input Purkinje cells receive *in vivo* via parallel fibers and interneurons, dynamic current clamping (dcc) was used to apply a baseline level of random synaptic inputs to these cells. The amount of simulated synaptic current injected ( $I_{inj}$ ) was calculated at a 10 kHz refresh rate from

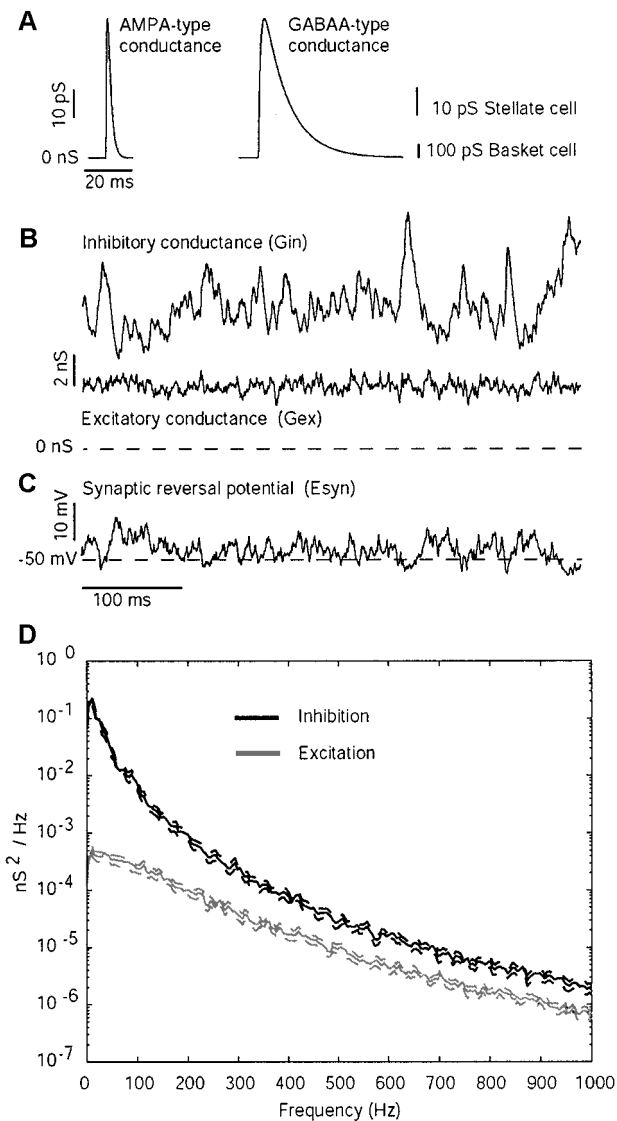


**Figure 2**

Construction of dynamic current clamp stimuli. (A) Waveform of a unitary AMPA EPSC and a unitary GABA IPSC. Basket and stellate cell IPSCs were identical except the maximal conductance used was 20 times larger for basket cell inputs. (B) The total excitatory and inhibitory conductance resulting from the addition of all unitary events (see Methods). The mean amplitude of the total synaptic conductance was 13.7 nS. Note that fluctuations in inhibition are greater than in excitation due to the presence of fewer, but larger randomly timed events. (C) The combined synaptic reversal potential ( $E_{\text{syn}}$ ) of excitation and inhibition. This potential describes the trajectory of  $V_m$  for which the net driving force of all synaptic input remains at 0, and thus no net synaptic current flows. Any deviation of  $V_m$  from this trajectory leads to a shunt current driving  $V_m$  back towards  $E_{\text{syn}}$ . (D) The power spectrum of inhibition (black lines) and excitation (gray lines) of 10 s of input conductances was computed using Matlab. The spectrum is debiased, i.e. the effect of the mean baseline conductance is removed. The dotted lines show the 95% confidence limits of the power spectrum. Note that the y axis is logarithmic, i.e. the power changes 10-fold between tick marks. Note that the power of inhibition is higher than that of excitation at all frequencies, and in particular that low-frequency fluctuations are 100-fold stronger in inhibition.

the recorded membrane potential ( $V_m$ ) and two stored synaptic conductance waveforms representing the sum of excitatory ( $G_{\text{ex}}$ ) and inhibitory ( $G_{\text{in}}$ ) conductances. The equation used to calculate synaptic current was:

$$I_{\text{inj}} = I_{\text{ex}} + I_{\text{in}} = G_{\text{ex}} * (E_{\text{ex}} - V_m) + G_{\text{in}} * (E_{\text{in}} - V_m),$$

where  $E_{\text{ex}}$  and  $E_{\text{in}}$  are the synaptic reversal potentials of 0 mV for excitation and -70 mV for inhibition respectively. A CIO-DAS 16/F analog-to-digital board (Computer Boards) attached to a computer using a customized software data acquisition program running under the DOS operating system was used to acquire data (see Gauck and Jaeger, 2000 for details). Recording electrodes were attached to an Axon HS2A 0.1 LU headstage and recordings were obtained with an Axoclamp 2B amplifier (Axon Instruments).

## Construction of synaptic inputs

The synaptic conductance traces  $G_{\text{ex}}$  and  $G_{\text{in}}$  were modeled to reflect expected *in vivo* excitatory and inhibitory inputs that Purkinje cells receive from parallel fibers and molecular layer interneurons respectively (see Jaeger and Bower, 1999, and Fig. 2). The mean amplitude of  $G_{\text{ex}}$  and  $G_{\text{in}}$  was in the lower range of conductance amplitudes employed in this previous study. This range of conductance levels and the reduction of electrode capacitance with Sylgard allowed the use of a single patch electrode for dynamic clamping without incurring feedback artifacts in the recorded membrane potential. Excitatory inputs were modeled as a pure AMPA conductance, since in mature Purkinje cells an NMDA component is not found with parallel or climbing fiber inputs.<sup>20</sup> Inhibition was simulated purely as a GABA-A conductance, since IPSCs elicited by interneuron stimulation are fully blocked by the selective GABA-A blocker bicuculline.<sup>21,22</sup> Individual AMPA and GABA<sub>A</sub> inputs were modeled as biexponential EPSCs and IPSCs using a GENESIS (<http://www.genesis-sim.org>) simulation. EPSCs had a rise time constant of 0.5 ms, decay time constant of 1.2 ms and a maximum conductance of 50 pS. This time course and amplitude was made to match experimental finding of parallel fiber synapses.<sup>23</sup> The total excitatory conductance waveform was constructed from 1000 AMPA synapses firing randomly at 36 Hz. This pattern is equivalent to 10,000 AMPA synapses firing at 3.6 Hz, or 100,000 AMPA synapses firing at 0.36 Hz. Recent findings on parallel fiber synapses suggest that many of the approximately 200,000 synapses a Purkinje cell receives may be silent.<sup>24</sup> The mean firing rate of granule cells *in vivo* has not been determined in awake animals, but may be around 3 Hz in anesthetized rats.<sup>25</sup> The IPSCs we incorporated in our dynamic clamp conductance had a rise time constant of 1 ms, a decay time constant of 10 ms matching published data<sup>22</sup> and a maximum conductance of 50 pS for stellate cells and 1 nS for basket cells. These values match the

amplitudes of small and large IPSCs found for unitary inhibitory events in Purkinje cells.<sup>26</sup> IPSCs elicited from interneurons closest to the Purkinje cell layer are considerably larger than IPSCs from more superficial interneurons,<sup>26</sup> though there is no physiological evidence for a binary distribution of Purkinje cell IPSC amplitudes elicited by stellate cell and basket cell input. A gradual decrease of IPSC amplitudes in Purkinje cells with increasing distance of presynaptic interneurons from the Purkinje cell layer fits well with anatomical data showing a similarly gradual transition between axonal termination patterns typically described for the ‘classical’ basket cell and stellate cell types, respectively.<sup>18</sup> Nevertheless, to reduce the number of parameters in the construction of our stimuli, we chose to represent inhibitory inputs along the classical binary division of basket and stellate cells. The total simulated inhibitory conductance waveform was made up of 500 stellate cell synapses and 50 basket cell synapses, which were all activated randomly at a mean rate of 10 Hz. Random activation times of excitatory and inhibitory inputs were selected with a random number generator (rand in GENESIS) with a fixed probability of activation at each time step, thus resulting in an exponential distribution in the activation of single synapses. The resulting relative balance of excitation and inhibition was suitable for controlling Purkinje cell spiking at physiological rates, which is only possible within a narrow range of relative levels of excitation and inhibition.<sup>5</sup> The balance of excitation and inhibition can be expressed in the combined synaptic reversal potential (Fig. 2C) during dynamic current clamping using the following equation:

$$E_{\text{syn}} = (G_{\text{ex}} * E_{\text{ex}} + G_{\text{in}} * E_{\text{in}}) / (G_{\text{ex}} + G_{\text{in}}).$$

Shunt currents ( $I_s$ ) due to the presence of background conductances  $G_{\text{ex}}$  and  $G_{\text{in}}$  are proportional to the distance of the membrane potential from  $E_{\text{syn}}$  at any time:

$$I_s = (G_{\text{ex}} + G_{\text{in}}) * (V_m - E_{\text{syn}}).$$

The total rates and amplitudes of excitatory and inhibitory input can not be fully constrained by available experimental data. To examine the effects of different amplitudes of background input, we used a variable gain factor of  $1\times$  or  $2\times$  on the baseline of conductances as in previous studies (5, 6). Increasing the conductance gain does not alter  $E_{\text{syn}}$ , but it increases the shunt current at a given driving force ( $V_m - E_{\text{syn}}$ ) proportionally. In Purkinje cells this effect leads to a slower spike rate when the gain of a baseline of excitatory and inhibitory input is increased because an intrinsic inward persistent current is shunted more effectively.<sup>5</sup> A slowing spike rate, however, would act as confounding factor in our quantification of spike pause responses due to additional inhibitory inputs elicited by electrical stimulation. Therefore, we employed a 2.5 mV positive shift in driving forces for both inhibition and excitation for clamp gain 2, which we empirically found to lead to a close match in mean spike rates in response to both gains for most neurons (see

Results). This manipulation depolarizes  $E_{\text{syn}}$  by a constant value of 2.5 mV, while leaving the waveforms and the relative balance of excitation and inhibition unchanged. We avoided the use of bias currents to adjust spike rates during stimulation, because such currents would introduce mechanism of triggering spikes independent of the trajectory of applied conductances. The relative amplitude and fluctuations between excitatory and inhibitory conductances ( $G_{\text{ex}}$  and  $G_{\text{in}}$ ) were very similar to our previous study (Fig. 1B in (5)). The power spectra of the inhibitory and excitatory conductances (Fig. 2D) show that the random input trains used result in a broad range of frequencies at which conductances fluctuated with a smooth falloff towards higher frequencies. At low frequencies the power of inhibitory conductances dominated 100-fold over excitatory conductances, which is due to the much higher total number of random EPSCs adding to a near flat conductance level (Fig. 2B). We found that the shape of the power spectrum of AMPA excitation and GABA-A inhibition is very similar for a large range of synaptic activation rates (not shown), but that the whole spectrum is shifted vertically to higher power when fewer and larger unitary events are present.<sup>27</sup>

## Data analysis

Acquired whole-cell recordings were analyzed with Matlab (The Mathworks, Inc.). A baseline spike rate was determined for each trial from 500 ms of spontaneous spiking or spiking controlled by dynamic clamping before inhibition was stimulated electrically. Trials with fewer than 4 spikes in the baseline period were discarded. Spike pauses elicited by electrical stimulation were quantified as the time from the first electrical stimulus in the train to the first action potential afterwards. Trials in which the pause lasted longer than 1 s were discarded, as a transition to a down-state likely occurred (see Fig. 3, and (28)). In addition, pauses following electrical stimuli that were given when Purkinje cells were in a spontaneous down-state were not analyzed. Besides the duration of spike pauses we quantified the peak hyperpolarization (IPSP) elicited by electrical stimulation in each condition. This value was derived from the average response over repeated trials using the same stimulus condition ( $n = 4-10$ ). The injected current during dynamic clamping was examined for shunt currents elicited by electrically stimulated inhibition. This analysis was performed by subtracting the injected current in the absence of electrical stimulation from the injected current after electrical stimulation. The applied dynamic clamp conductance was identical under both conditions, and results from 4–10 trials were averaged. The quantitative measurements were analyzed statistically using the Systat software package (SPSS, Inc.).

A custom-written C-routine was used to analyze the precision of spike timing over repeated trials using the

same pattern of input conductances (see Fig. 4). The spike times in each trial were compared against the closest matching spike times in all other trials. A histogram of the spike timing accuracy across trials was constructed (precision histogram), and compared to the chance level of expected spike coincidences determined from 100 repetitions of shuffling the spike-intervals of the source trials. This method is a refinement of the cross-correlation method we have employed previously,<sup>6</sup> but it is improved in the sense that each spike in the source trace is only matched to a single spike in the target trace if present within the target window.

## Results

### Spontaneous activity

Previous studies have shown that spontaneous spiking of Purkinje cells *in vitro* consists of ongoing irregular spiking, in which small pauses are caused by inhibitory inputs from local interneurons.<sup>5,10</sup> The recording conditions in this study were different in that all excitatory synaptic input in the slice was blocked pharmacologically. Nevertheless voltage clamp recordings of Purkinje cells typically showed an ongoing baseline of spontaneous IPSCs (Fig. 3A), indicating that inhibitory interneurons were active in the absence of excitatory input under our recording conditions. In current clamp, Purkinje cells showed an ongoing irregular pattern of spiking (Fig. 3B), indicating that intrinsic inward plateau currents can keep the cell in a spiking up-state, which shows spontaneous spiking with brief pauses that are presumably due to the inhibitory background inputs. In some Purkinje cells, recordings infrequently dropped into spontaneous down states (Fig. 3C), which lasted several seconds. This rare display of bistability is in agreement with a recent study showing the stabilization of the up-state by I-H.<sup>28</sup> The down-state could also be elicited with a hyperpolarizing bias current. Additional small hyperpolarizing current pulses (80 pA, 100 ms) were used to determine the effective input resistance in the down-state, which was found to be  $56 \pm 13 \text{ M}\Omega$ . The input resistance in the up-state could not be determined cleanly with current pulses due to ongoing spike activity. It was substantially lower than in the down-state, however, as indicated by much smaller deflections in membrane potential with small 10 ms current pulses than found in the down-state.

### Electrical stimulation of basket and stellate cells

We generally adjusted the stimulation amplitude until a small but consistent spike pause was observed in current clamp for single pulse stimulation (Fig. 3B). When recordings were switched to voltage clamp, the same stimulation intensity resulted in an IPSC (Fig. 3B). The amplitude of a response to a single electrical stimulus was comparable to spontaneous IPSCs or spike pauses,

indicating that only one or a few inhibitory inputs were stimulated. The average stimulation strength to elicit a small spike pause was  $47 \pm 18 \text{ V}$  (mean  $\pm$  standard deviation) for upper ML stimulation, which was significantly higher than the average stimulation strength of  $39 \pm 17 \text{ V}$  for deep ML stimulation in the same population of 13 Purkinje cells ( $p < 0.05$ , paired t-test). Because stimulation strength may not directly correspond to the number of stimulated axons due to a different density or stimulation threshold of axons in the upper and deep ML, we can make no quantitative statements as to the relative strength of stellate cell vs. basket cell inhibition. A qualitative jump in responses suggesting a fundamentally different effect of basket cell versus stellate cell inhibition was not observed, however.

A brief train of 2–5 stimulation pulses at 200 Hz increased the amplitude of the elicited IPSC in voltage clamp severalfold (Fig. 3B) and led to a prolonged spike pause in current clamp. It is important to note that the spike pause duration could far exceed the duration of the IPSC, which suggests that spike pauses were prolonged via the deactivation of the sustaining inward plateau current. Although the membrane time constant also effects a slowing of repolarization and a thus a prolongation of IPSP duration in comparison to IPSC duration in voltage clamp, this effect can not account for pauses lasting several hundred milliseconds. In fact, in some cases a strong stimulus could switch the Purkinje cell into a down-state (Fig. 3C) given by a long-lasting deactivation of inward plateau currents, as previously observed.<sup>28</sup> The spike pause durations were quantified for inhibitory input from presumed basket cells (stimulation in lower 1/3 rd of molecular layer (Deep ML),  $n = 18$ ) and presumed stellate cells (stimulation in upper 1/3 rd of molecular layer (Upper ML),  $n = 29$ ) activation (Fig. 3D). In both cases, the pause duration significantly increased between 1 and 3 pulses of stimulation, but did not further increase between 3 and 5 pulses. This finding suggests that brief bursts of 2–4 spikes of interneurons *in vivo* may provide a preferred strong input condition different from an irregular single spike mode.

### Control of spontaneous activity by dynamic current clamping

We have previously shown that the random background of many excitatory and inhibitory inputs that a Purkinje cell is expected to receive *in vivo* can exert a tight control over the rate and timing of action potentials.<sup>5,29</sup> In the previous work the effect of dynamic clamping was examined in isolation while all endogenous synaptic input was blocked. In the present study we left endogenous inhibitory input intact, and examined the interaction between it and additional conductances applied with dynamic clamping. This approach allows us to examine the important question of how the effect of synaptic

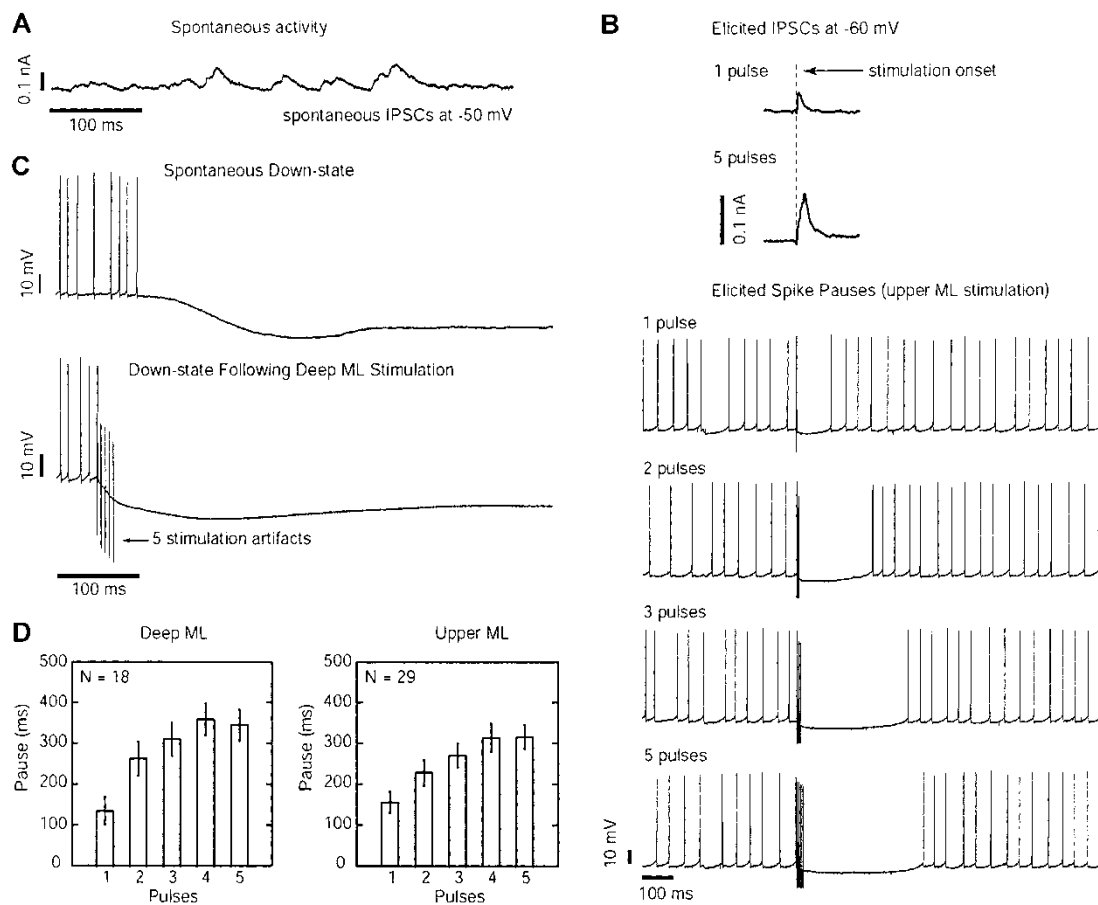


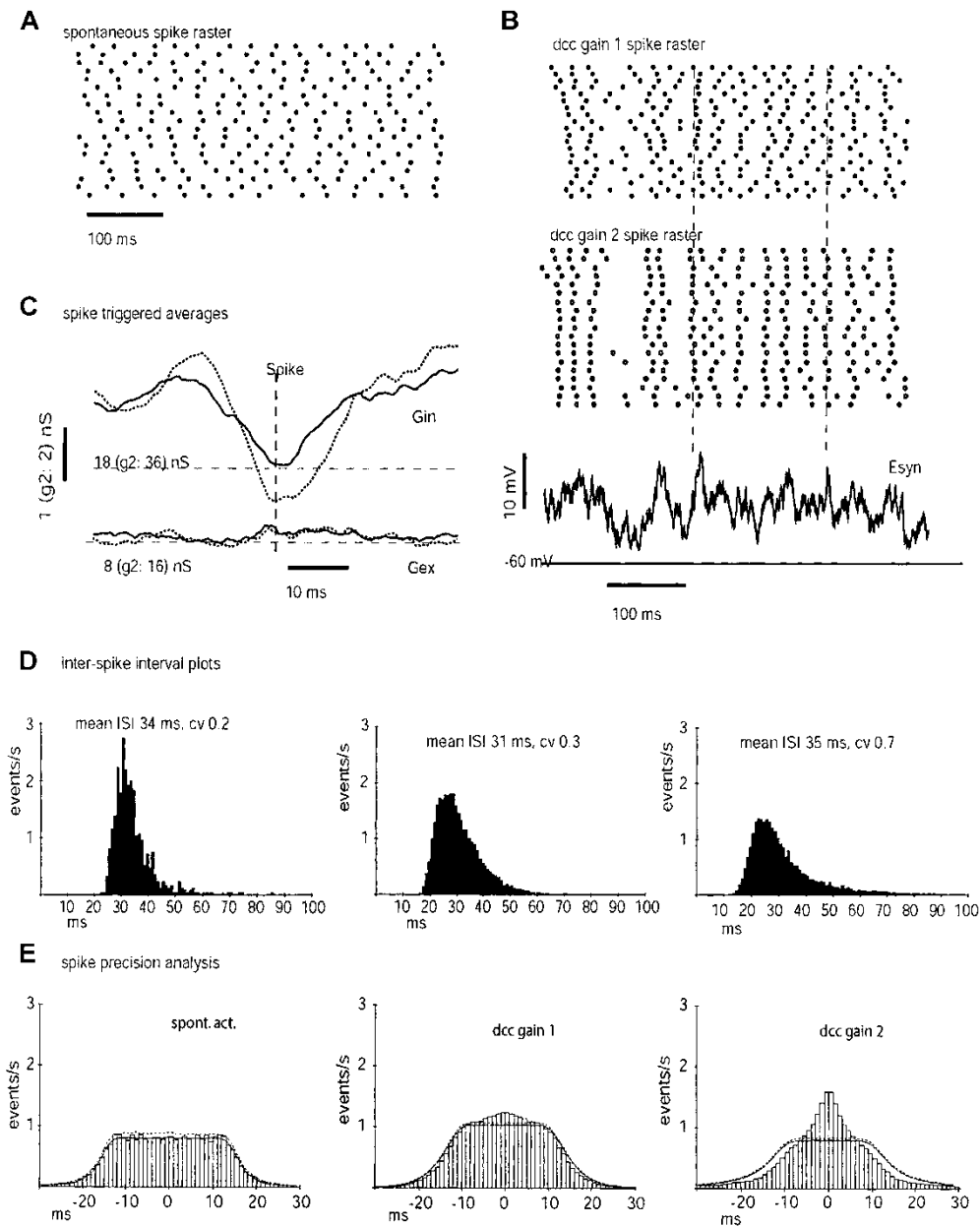
**Figure 3**

Effects of electrical stimulation on spontaneous spiking activity in Purkinje cells. (A) Example of spontaneous IPSCs recorded in voltage clamp, indicating that interneurons are active when excitatory input in the slice was blocked. (B) Electrical stimulation of inhibitory interneurons elicited a stimulus locked IPSC in voltage clamp (top) and a pause in Purkinje cell spontaneous spiking in current clamp (bottom). The size of the IPSC and the duration of the pause increased for stimulation trains with multiple pulses at 200 Hz. Note that the duration of pauses could far outlast IPSCs recorded in voltage clamp, suggesting that the pause duration was prolonged by the deactivation of voltage-gated inward plateau currents. Also note that the background spiking itself was irregular, presumably due to the background of spontaneous inhibitory input shown in (A). (C) During spontaneous activity Purkinje cells sometimes dropped into a non-spiking down-state (top trace). Cells resumed spiking after a variable period, usually lasting less than 10 seconds. Following electrical stimulation of inhibitory inputs (5 stimuli at 200 Hz in this example), Purkinje cells could be pushed into a down-state with identical characteristics (bottom trace). This is likely the result of deactivating inward plateau currents below a critical threshold. (D) Average pause duration in ms was calculated for pulse trains of stimulation 1–5 pulses at 200 Hz. Results are subdivided for deep ( $n = 18$  cells) and upper ( $n = 29$  cells) ML stimulation sites. Stimulations that caused a transition into a down-state were excluded from scored data.

inputs is influenced by the presence of an in-vivo like background.

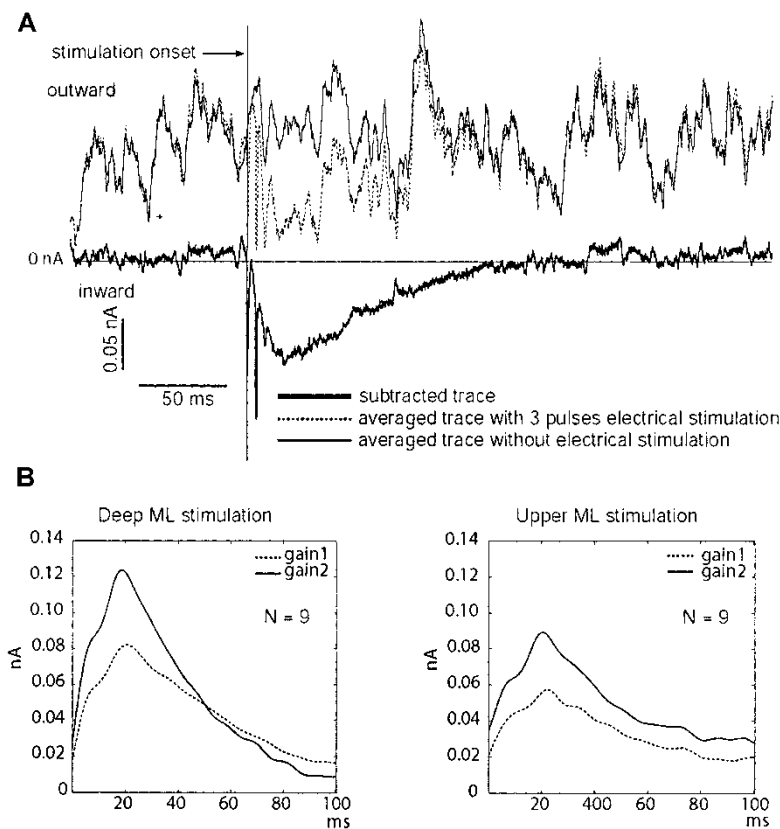
Both in the absence and presence of dynamic clamping Purkinje cell recordings were characterized by ongoing irregular spiking (Fig. 4A,B). In the absence of dynamic clamping a small hyperpolarizing bias current (between 0 and  $-0.3$  nA) was given to reduce the spike rate to values comparable to those seen with dynamic clamping and to increase long-term stability of recordings. Any bias current was switched off during presentation of dynamic clamp stimuli, and the spiking was controlled by conductance inputs alone. Both spontaneous spiking and spiking during dynamic clamping showed a smooth interspike interval (ISI) distribution with a single mode and a tail indicating the presence of a small proportion of

prolonged ISIs (Fig. 4D). The autocorrelation histograms were flat, indicating the absence of oscillatory spiking (not shown). A spike precision analysis was carried out to determine how well spikes were aligned across repeated trials of the same stimulus condition (Fig. 4E). A shuffle predictor was used to estimate the number of spikes that would be aligned with each other by chance alone given the specific ISI distribution. In the case of spontaneous spiking the shuffle predictor (solid line) is identical with the precision histogram indicating that subtraction of the shuffle predictor successfully eliminated any spike alignments occurring by chance. For dynamic clamping at gain 1 (average total synaptic conductance of 13.7 nS) a clear central peak emerged in the precision histogram, which was much more



**Figure 4**

The control of spiking by dynamic clamping. (A, B). Spike raster plots of spontaneous activity, and activity recorded during dynamic clamping. Each line in the raster plots represents a trial with the same applied conductance pattern depicted below as  $E_{syn}$  (see Methods). As the applied conductance amplitudes increased, more spikes were aligned with depolarizing deflections in  $E_{syn}$  (gray dashed lines are drawn for two clear examples). (C) Spike triggered averages of the applied conductances were constructed from repeated trials of 20 s of dynamic clamping. The result indicates that spike timing was controlled more by a transient decrease in inhibition than by an increase in excitation given the input statistics depicted in Fig. 2. (see (5), for more details). Spike-triggered averages for gain 1 dynamic clamp stimuli are shown as solid lines, and for gain 2 stimuli as dotted lines. Note that the y-axis scale is adjusted by a factor of 2 for the spike triggered averages of gain 2 stimuli so that the slightly increased amplitude of the spike triggered average reflects a change in the relation of spike timing to the waveform of the dynamic clamp conductance, and not the increase in conductance amplitude. (D) The inter-spike interval plots show that the objective of keeping a similar spike rate across conditions was well met for this cell. At the high clamp gain, however, spike-interval variability increased as indicated by a broadening of the interval distribution and by the increase in the coefficient of variation (cv). (E) Spike precision histograms were constructed by plotting the alignment of all spikes across all pairwise combinations of trials (see Methods). The solid line represents the chance distribution of spike alignments and the dotted line represents 3 standard deviations from this chance distribution. The superimposition of the solid line with the histogram for the case of spontaneous spiking demonstrates the successful estimate of chance events with our shuffle predictor. At the doubled gain of clamp conductance, a larger number of spikes was aligned more precisely across trials.

**Figure 5**

The shunt current resulting from electrical stimulation of interneurons. (A) The current caused by dynamic clamp conductances without additional electrical stimulation (thin solid line) was subtracted from the current induced by the same conductance pattern in the presence of electrical stimulation (dotted line). As the electrical stimulation caused a hyperpolarization, the driving force for dynamic clamp current increased, and thus induced a shunt current. The subtracted trace (solid line) reveals the time course and amplitude of shunt current. Traces shown are averages from multiple trials aligned to the same stimulation time. Current spikes due to action potentials were digitally removed before the average was constructed. (B) Averaged shunt currents for 9 stimulation times at 2 s intervals over 20 s of dynamic clamping are shown ( $n=9$  neurons,  $n=81$  responses). For each neuron, deep and upper ML stimulation was performed, and the resulting shunt current is plotted separately.

prominent when the gain of the clamp conductance was doubled (Fig. 4E). A quantitative analysis of 14 cells showed that the average spike rate was nearly constant between clamp gain 1 ( $35.7 \pm 12.2$  Hz) and gain 2 ( $34.4 \pm 16.3$  Hz) as intended by our stimulus design using a 2.5 mV offset in driving forces for gain 2 stimuli (see Methods). The average rate of spikes timed precisely within  $\pm 2$  ms across trials (after subtraction of chance level) increased significantly from 2.9 Hz to 5.7 Hz ( $n=14$ ,  $p=0.001$  paired t-test). Two vertical dotted lines in Fig. 4B show examples of stimulus conditions that led to aligned spike events. As previously described<sup>5</sup> these conditions mainly consist of a phasic decrease in inhibition preceding the spike (Fig. 4C) that leads to a depolarization of the membrane potential to which the cell is pushed by the input. These results indicate that dynamic clamping takes partial control of the spike pattern in the case of ongoing endogenous IPSCs, and that short phasic changes in the input conductance lead to well aligned spikes even in the presence of additional noise conductances.

### The IPSCs from interneurons are partly shunted by dynamic clamp conductances

We electrically stimulated interneurons during a random conductance background applied with dynamic clamping. Nine electrical stimulus pulses (or brief pulse trains) were applied with 2 s intervals over 20 s of a dynamic

clamp stimulus. The identical random conductance pattern was applied to all neurons in the absence and in the presence of electrical stimulation of inhibitory inputs. Using this method we can determine the time course and amplitude of the current that is shunted by the continuous background dynamic clamp conductances when inhibition is elicited with electrical stimulation. The current that the dynamic clamp injects is given by  $I_{dc} = (G_{ex} + G_{in}) * (V_m - E_{syn})$ . The stimulation of inhibitory inputs leads to a hyperpolarization of  $V_m$ , which changes the driving force of the clamp current ( $V_m - E_{syn}$ ). The change in driving force leads to a change in clamp current that counteracts the stimulation-elicited current (see Methods for details). When the dynamic clamp current in the absence of electrical stimulation is subtracted from the dynamic clamp current with electrical stimulation, the shunted component of the stimulation-elicited current is revealed (Fig. 5A). It should be noted that the shunt current of the background synaptic conductances counteracts components of stimulated synaptic current as well as other membrane currents that are changed during an IPSP. As described above, in Purkinje cells this most likely includes shunting an outward current caused by the deactivation of inward plateau currents. We quantified the average shunt current elicited by the 9 stimulation pulses in our 20 s dynamic clamp period in 9 neurons ( $N=81$  events). This analysis was carried out for 2 amplitudes of background conductance (see Methods regarding dynamic clamp gain), and for stimulation in the deep or upper molecular layer

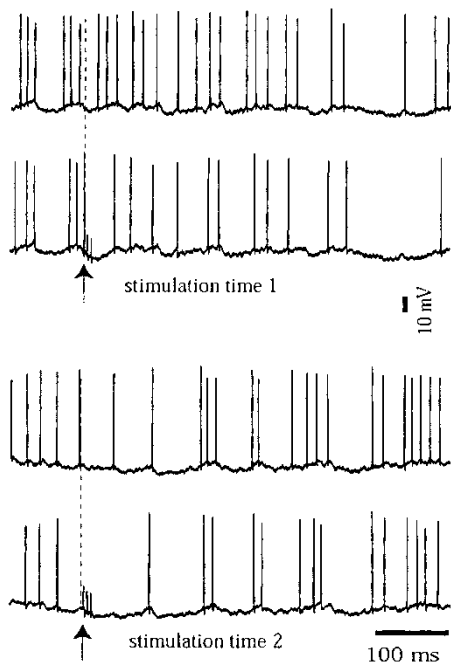


**Figure 6**

Electrical stimulation of interneurons during dynamic clamping induces short spike pauses. Two examples of comparing spike trains with and without electrical stimulation (indicated by arrows) are shown. The examples differ by the random sequence of background inputs provided by dynamic clamping. The spike pause induced by electrical stimulation could be short (top two traces) or long (bottom example) depending on the background input condition.

(Fig. 5B). The data show that electrically stimulated IPSCs were shunted more when the level of background input conductances was increased. Both the peak shunt current and the total shunted charge (integral of shunt current) were significantly greater for a high-conductance of background inputs (dynamic clamp gain 2 vs gain 1, *t*-test,  $p < 0.02$ ). The peak shunt current was also significantly larger for deep ML than upper ML stimulation ( $p < 0.01$ ), indicating that basket cell input had a stronger effect on  $V_m$  at the soma than stellate cell input. Shunting of presumed basket cell stimulation also differed from presumed stellate cell stimulation in that the decay time of the shunt current was faster at the higher clamp gain. This suggests a somatic source of the shunted conductance, as the somatic shunt current elicited by a somatic dynamic clamp will more effectively eliminate a local hyperpolarization, and thus reduce a somatic change in driving force more quickly than a dendritic source.

### Electrical stimulation of interneurons during dynamic current clamp produces short spike pauses

For the same set of stimulus conditions analyzed above for shunt currents we could examine the spike pattern in the recorded voltage traces. Figure 6 shows the response

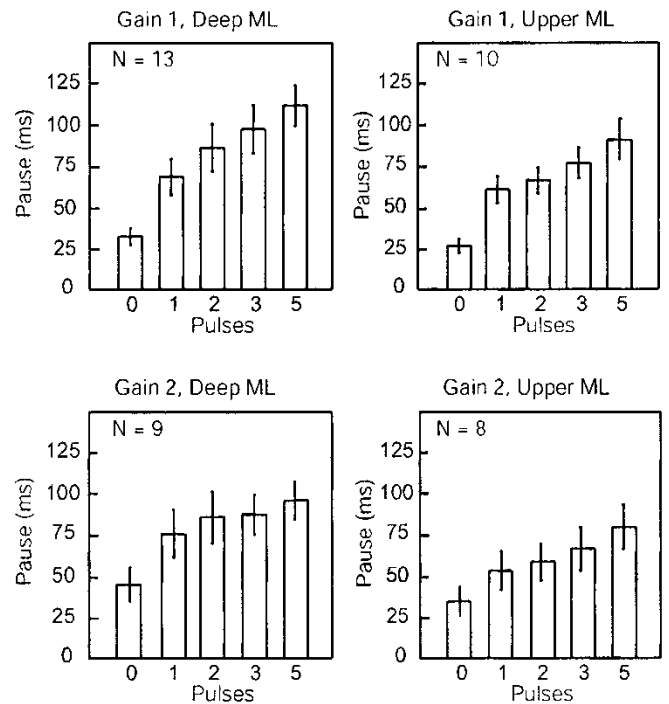


**Figure 7.** Quantification of spike pauses elicited by upper and deep ML stimulation for 1–5 pulses (at 200 Hz) of interneuron activation. The results show the average pause duration from 9 stimulation times during dynamic clamping ( $n = 8$ –13 neurons depending on stimulus condition). The upper panels show spike pauses elicited when the background inputs had half the amplitude (gain 1) than in the bottom panel (gain 2).

of a typical recording to a brief train of interneuron stimulation (3 pulses at 200 Hz) for two of the 9 different stimulation times during our 20 s dynamic clamp episode. In each case, a brief spike pause was elicited when compared to the baseline spike pattern without electrical stimulation. The average spike pause for all 9 stimulation times was quantified for the recorded populations of cells as a function of dynamic clamp gain and upper or deep molecular layer stimulation (Fig. 7). As for electrical stimulation during spontaneous spiking (Fig. 3) deep compared to upper molecular layer stimulation and an increase in the number of stimulation pulses (at 200 Hz) led to a longer spike pause. Both the total pause duration and the increase in duration with more stimulation pulses were much reduced compared to the effect during spontaneous spiking, however. For example, the stimulus condition of 3 deep ML pulses resulted in an average pause duration of  $363 \pm 205$  ms during spontaneous spiking, and for the same population of 9 cells the pause was significantly reduced to  $108 \pm 58$  ms during dynamic clamping at gain 1 (paired *t*-test,  $p = 0.003$ ). Dynamic clamping at gain 2 further reduced the average pause duration to  $88 \pm 34$  ms in this population of cells, but this additional decrease did not reach significance. The demonstration of the shunted IPSC current above makes it clear that one of the underlying mechanisms is synaptic shunting. Other effects, however, could contribute as

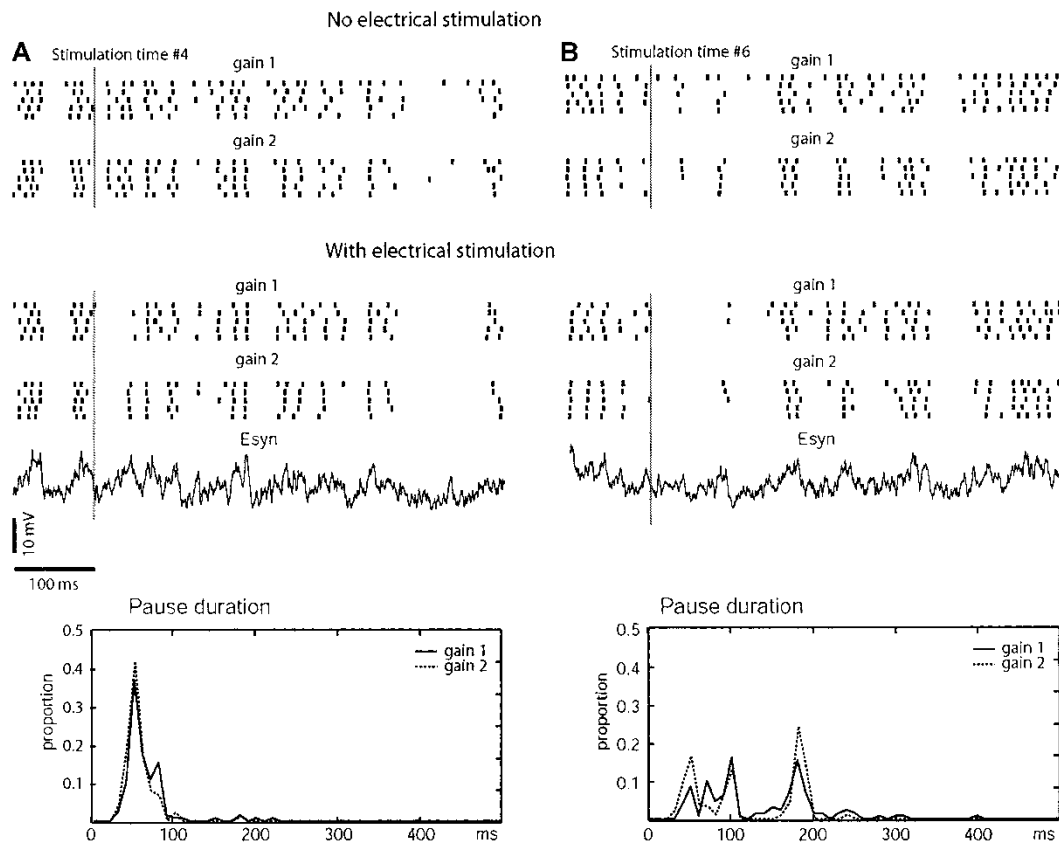


**Figure 8**

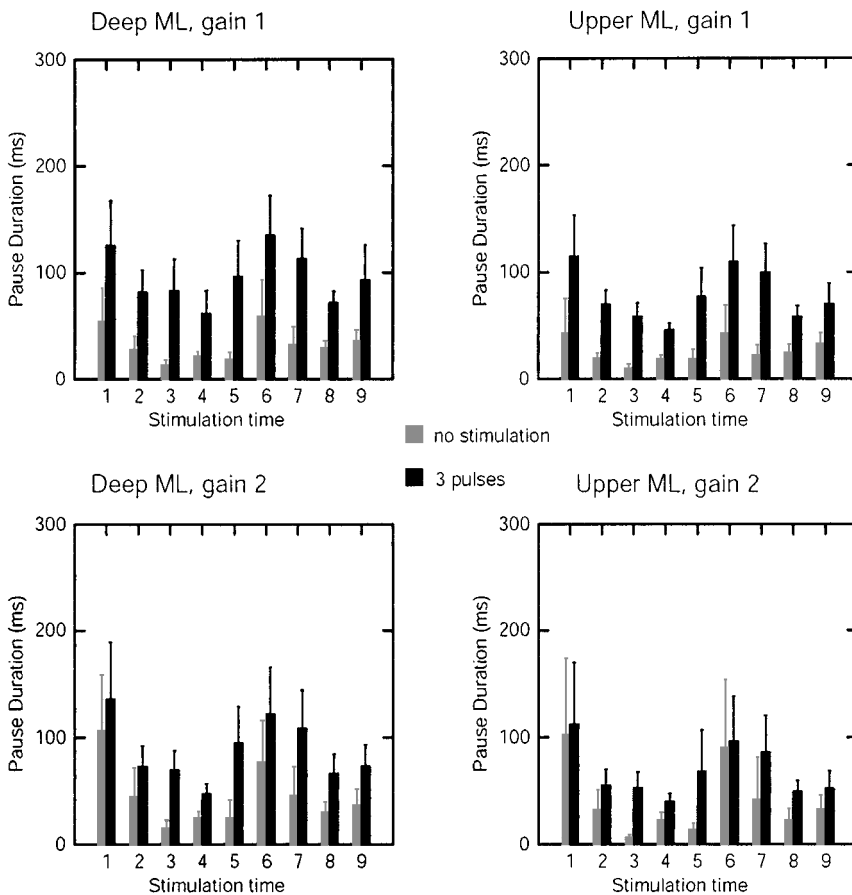
Spike pause duration was controlled by the pattern of background inputs. Spike raster plots across repeated trials are shown in the absence and presence of electrical stimulation (3 pulses at 200 Hz) for a typical neuron. The  $E_{\text{syn}}$  trace shows the trajectory of the combined reversal potential of excitation and inhibition. The results of two different stimulation times are compared between A and B. The spike pause distribution for these stimulation times sampled from 8–13 neurons is plotted below for both clamp gains.

well. In particular, it is likely that the deactivation of intrinsic plateau currents also contributed to the pause duration in response to strong inhibitory inputs (Fig. 3). This hyperpolarization-induced deactivation is reduced by background synaptic input, which tends to keep the membrane depolarized at  $E_{\text{syn}}$  (see Methods and (6)). As described below, beyond the average level of dynamic clamp conductance, specific fluctuations in this conductance significantly determined the duration of pauses following a stimulation-elicited pulse of inhibition. This effect is particularly interesting, in that it allows specific new synaptic information to modulate the time course of the response to previous input.

### Fluctuations in background activity control spike pause duration

As shown in Figure 4 and (5), transient fluctuations in the input conductance can control individual spikes precisely. *In vivo*, such fluctuations are likely to correspond to ongoing information from sensory input and intrinsic processing. The timescale over which inputs can interact in a single neuron has important implications for signal

processing. In Purkinje cells, intrinsic dynamics can lead to prolonged responses both for strong inhibitory inputs (Fig. 3B), and for excitatory inputs.<sup>30</sup> Here, we examine how inhibitory responses are influenced by fluctuations in the surrounding input conductances (Figs. 8, 9). We find that specific fluctuations in the background conductances have a strong influence on the expression of the inhibitory response. Stimulation at two typical times in the background input pattern are illustrated in Figure 8. At both stimulation times some spikes due to peaks in the background input (time course given by  $E_{\text{syn}}$ ) were eliminated due to the inhibitory input compared to the baseline condition (Fig. 8A, top panel). However, the induced pause only lasted 46 (gain 2: 39) ms on average at stimulation time 1, but the same stimulus elicited an average pause of 123 (gain 2: 109) ms at stimulation time 2. Moreover, the distribution of pause times was not smooth, but showed distinct termination times (bottom panel). These pause termination times correspond to specific fluctuations in the background conductance pattern that lead to transient membrane depolarization. Stronger such fluctuations soon after the inhibitory stimulation can terminate a spike pause early. Beyond the time of pause termination there was little or no

**Figure 9**

Distribution of pause durations elicited at 9 different times (with 2 s intervals) of the dynamic clamp background. Black bars show the distribution of the pause (time to first spike) following 3 pulses of electrical stimulation at 200 Hz. Gray bars show the distribution of times until the first spike occurred when no electrical stimulation of interneurons was given at the same times in the dynamic clamp background. For each stimulus time, the additional pause induced by interneuron activation is the difference in height between black and gray bars. The error bars denote the 95% confidence level for each distribution, and non-overlapping error-bars indicate a statistically significant difference in bar height ( $p < 0.05$ ). Note that at clamp gain 2 significances were generally reduced and at some stimulation times interneuron activation did not lead to a significant pause. This is indicative of increased shunting at gain 2.

persistence of the inhibitory inputs in affecting spike timing. This can be verified by comparing the spike rasters following pause termination between trials with or without electrical stimulation (Fig. 8).

We analyzed pause durations quantitatively for 9 different stimulation times as a function of dynamic clamp gain, and deep vs. upper ML stimulation (Fig. 9). In general, a significant spike pause was induced by the stimulus. However, only spikes occurring within approx. 100 ms after stimulation could be eliminated from the background spike pattern. The termination time of the pause was more tightly controlled at some stimulus times (small error bar in Fig. 9) than others. Well-timed termination in the spike pause was caused by a strong depolarizing fluctuation in the background input between 50 and 100 ms after electrical stimulation (Fig. 8A), whereas the absence of such a strong trigger for pause termination lead to variable duration in the pause (Fig. 8B). The interaction of presumed stellate cell stimulation (upper ML) with the background conductances was quite similar to presumed basket cell stimulation, except that pauses were generally shorter. Overall, these data indicate that beyond the effect of shunting to shorten stimulation responses, which is proportional to the level of background conductances, specific fluctuations in the input pattern can terminate pause responses at well defined times. A flexible control of pause offsets could be related

to an adaptive timing function often assumed to be carried out in cerebellar cortex.

## Discussion

The pioneering theory of James Albus (13) hypothesized that specific pauses in Purkinje cell activity would trigger activation of neurons in the deep cerebellar nuclei via disinhibition, and thus constitute a motor command. While Albus thought that pauses in Purkinje cell activity are caused by a weakening of excitatory input synapses, the best physiological evidence for pauses in Purkinje cell activity implies the activation of inhibitory inputs from interneurons.<sup>10,30</sup> These two mechanisms are not mutually exclusive, however, and recent evidence points to the presence of plasticity of the synapses onto interneurons<sup>31</sup> as well as a joint action of excitatory and inhibitory synapses on learnt behavioral Purkinje cell responses to sensory stimulation *in vivo*.<sup>32</sup> In general, Purkinje cells can show strong transient responses to sensory stimulation consisting both of excitatory and inhibitory components.<sup>33,34</sup> Purkinje cell responses can be entrained during behavior,<sup>32,35,36</sup> and are likely needed in the adaptive control of motor performance. To optimally code the complex sensory environment in Purkinje cell activity it has been hypothesized that direct Purkinje cell

responses to a particular stimulus are modulated by the context of sensory inputs received from different somatotopic areas.<sup>12</sup> This modulation could be carried out by activity in the parallel fiber system, which originates from a wide band of granule cells in the medio-lateral axis reflecting different somatotopic inputs. The present study shows how the mechanism of synaptic shunting can lead to a gain control of specific sensory or motor responses. In essence, this mechanism evaluates the salience of a specific input among surrounding stimuli, and leads to a diminished response if the input was not of sufficient relative strength. Thus the effect of a given stimulus could be normalized to the ongoing background of 'noise' stimuli. Although the present study focused on the shunting of inhibitory inputs, the same mechanisms also apply to excitatory inputs and can effectively gate excitatory Purkinje cell responses, as recently shown in a modeling study.<sup>37</sup>

### The use of dynamic clamping as a simulation of the *in vivo* condition

In an isopotential compartment, the amount of shunt current provided by a baseline of synaptic conductances ( $G_{\text{syn}}$ ) is given by  $I_{\text{shunt}} = G_{\text{syn}} (V_m - E_{\text{syn}})$  as explained in more detail in the Methods section. We simulated the shunting properties of baseline conductances expected *in vivo* with a dynamic clamp conductance applied *in vitro*. Three questions clearly need to be addressed before our findings can be interpreted as reflecting the functioning of synaptic baseline conductances *in vivo*: (1) Is the background synaptic conductance *in vivo* of high enough amplitude to create shunt currents that significantly influence signal processing, and were the conductance levels applied with dynamic clamping realistic? (2) Is the use of focal dynamic clamp input at the soma a legitimate representation of distributed dendritic and somatic input occurring *in vivo*? (3) Are the observed results dependent on details of statistical fluctuations in input conductances that may not be realistic?

(1) Unfortunately, experimental data are not available to directly answer the question as to how large background synaptic conductances *in vivo* are, but a range of likely values can be estimated (see Methods). To lead to significant deflections in membrane potential synaptic conductances must be at least of similar size as the sum of all other conductances open in a neuron at a given potential. We measured the input conductance of recorded Purkinje cells to be 18 nS on average in the down-state, and higher in the up-state. The average conductance of our dynamic clamp conductance was 13.7 nS at gain 1, and 27.4 nS at gain 2. These values are at the lower range of conductances capable of controlling spiking behavior (Fig. 4, see also (5)), and at the lower range of estimates of conductances likely to occur *in vivo*. Thus, the synaptic shunting observed in the present study is expected to be at the low end of the actual situation *in*

*vivo*. A severalfold increase in total conductance due to synaptic input has recently been described in cortical pyramidal neurons,<sup>38</sup> indicating that the situation described here for cerebellar Purkinje cells is also applicable for other large neurons in the brain that receive thousands of inputs each second.

(2) The question as to the effect of distributed dendritic input *in vivo* compared to focal somatic input with dynamic clamping can be addressed by theoretical considerations and computer simulations. Cable theory shows that voltage attenuation in dendritic trees is strongly frequency dependent, and is greater from distal towards proximal locations than from the soma out.<sup>39</sup> For a constant baseline of somatic conductance the attenuation of voltage towards the distal dendrites is only around 10% for a sealed-end dendrite with a total electrotonic length of 1 lambda.<sup>39</sup> The maximal dendritic length of an active Purkinje cell is likely to be smaller than 1 lambda based on modeling results.<sup>40</sup> These considerations explain why dendritic plateau currents can be controlled in a similar way with a purely somatic conductance source or a distributed dendritic current source in our active Purkinje cell model.<sup>29</sup> In a direct simulation of synaptic shunt currents in a Purkinje cell model, we also found that a somatic conductance provided a similar shunting effect as a distributed synaptic input did.<sup>41</sup> For fast transient currents these considerations are not valid, however, and specific dendritic integration mechanisms such as dendritic spiking in response to a large local EPSC can not be simulated with a dynamic clamp at the soma due to a much reduced space constant for fast signals. Inhibitory synaptic currents, however, have relatively slow time constants, and can be similarly shunted by either the presence of a pure somatic or a distributed dendritic conductance.

(3) No data are available currently to answer the question what the specific fluctuations in excitatory and inhibitory conductances are *in vivo*, and how much excitation and inhibition are coupled. Therefore we assume that all inputs are random and independent of each other, which approximates a background 'noise' in the system, but not specific signaling. This background input can be described by its total conductance amplitude, and by the trajectory of  $E_{\text{syn}}$ , the combined reversal potential of excitation and inhibition. The objective of this study was to examine how the amplitude and fluctuations of this random background input modulate the responses to specific inhibitory input bursts. Such a modulatory action by the background input seems inescapable in Purkinje cells *in vivo*, which receive massive numbers of inputs. Our finding that the amplitude of background inputs modulates the duration of inhibitory signals suggests that overall activity level in the parallel fiber system may provide a suitable signal to gate the responses to specific inputs. This mechanism does not preclude the possibility of further specific interactions between different signaling inputs, which indeed are

likely to occur in cerebellar cortical processing. However, our findings are not restricted to the specific choice of input rates and EPSC/IPSC amplitudes we made, as the summed conductance of multiple random input trains retains a similar broad-band power spectrum (Fig. 2D) across a wide range of input conditions that could be considered realistic for Purkinje cell inputs.

### The role of basket and stellate cells in mediating inhibitory Purkinje cell responses

Inhibitory interneurons in cerebellar cortex are traditionally grouped into two classes.<sup>19</sup> In the outer molecular layer stellate cells send distributed axonal projections to Purkinje cell dendrites, and in the inner molecular layer basket cells send focused axonal projections to the axon hillock and soma of Purkinje cells, as well as ascending axonal projections to Purkinje cell dendrites. Physiological differences between stellate and basket cells have not been described to date, however. The anatomical dichotomy itself is not total, as a continuous gradient of axonal projection patterns can be found between outer and inner molecular layer interneurons.<sup>18,19</sup> In the present study we found no evidence for a clear dichotomy of interneuron function. Similar spike pauses in Purkinje cells could be elicited from inner and outer molecular layer interneurons and the responses at both sites were gated by background conductances. Activation of presumed basket cells on average triggered a stronger response, however, supporting the notion that inner molecular layer interneurons make a strong contribution to Purkinje cell spike pauses. At all stimulation sites brief trains (2–3 pulses at 200 Hz) of interneuron activation were most efficient in triggering spike pauses, suggesting that brief bursts of granule cell activity may be a favorable stimulus triggering interneuron activation. Bursting appears to be a common mode of granule cell activation in distinct

somatotopically arranged patches by sensory stimulation in the behaving rat,<sup>11</sup> and molecular layer interneurons react with fast bursts of their own to such granule cell input bursts.<sup>27</sup> Such interneuron responses are likely the cause for inhibitory sensory responses found in Purkinje cells overlying and surrounding areas,<sup>34</sup> and is thus likely to contribute significantly to disinhibition of neurons in the deep cerebellar nuclei.

### General significance of shunting in neural computation

Our findings in the present study are in agreement with previous studies suggesting that the amount of ongoing network activity influences the impact of a single synaptic input.<sup>1,10,38</sup> While we focused on the effect of synaptic shunt currents, which are proportionally larger with increased synaptic conductance amplitudes, the same increase in input conductance also leads to a reduction of the membrane time constant of the neuron. A modeling study of a pyramidal cortical neurons showed that the reduction in time constant in particular can lead to a sharpening of the time window in which an excitatory input volley triggers a spike.<sup>1</sup> In contrast to spike triggering by excitatory input volleys, the effect of an inhibitory input volley is more graded and prolonged. Thus the effect of a shortened time constant with increased background input is likely of much less significance for the processing of inhibitory input volleys. Our findings show, however, that the synaptic shunt current caused by background inputs is highly significant in modulating spike pauses caused by strong inhibitory inputs.

### Acknowledgements

This work was supported by NIMH grant MH57256.

## References

- Bernander O, Douglas RJ, Martin KAC, Koch C. Synaptic background activity influences spatiotemporal integration in single pyramidal cells. *Proc.Natl.Acad.Sci.USA* 1991; 88: 11569–11573.
- Paré D, Shink E, Gaudreau H, Destexhe A, Lang EJ. Impact of spontaneous synaptic activity on the resting properties of cat neocortical pyramidal neurons in vivo. *J Neurophysiol.* 1998; 79: 1450–1460.
- Ulrich D, Huguenard JR. Gaba(a)-receptor-mediated rebound burst firing and burst shunting in thalamus. *J Neurophysiol* 1997; 78: 1748–1751.
- Borg-Graham LJ, Monier C, Frégnac Y. Visual input evokes transient and strong shunting inhibition in visual cortical neurons. *Nature* 1998; 393: 369–372.
- Jaeger D, Bower JM. Synaptic control of spiking in cerebellar Purkinje cells: dynamic current clamp based on model conductances. *J Neurosci* 1999; 19: 6090–6101.
- Gauck V, Jaeger D. The control of rate and timing of spikes in the deep cerebellar nuclei by inhibition. *J Neurosci.* 2000; 20: 3006–3016.
- Rudolph M, Destexhe A. A fast-conducting, stochastic integrative mode for neocortical neurons in vivo. *J Neurosci* 2003; 23: 2466–2476.
- Chance FS, Abbott LF, Reyes AD. Gain modulation from background synaptic input. *Neuron* 2002; 35: 773–782.
- Mitchell SJ, Silver RA. Shunting inhibition modulates neuronal gain during synaptic excitation. *Neuron* 2003; 38: 433–445.
- Häusser M, Clark BA. Tonic synaptic inhibition modulates neuronal output pattern and spatiotemporal synaptic integration. *Neuron* 1997; 19: 665–678.
- Hartmann MJ, Bower JM. Tactile responses in the granule cell layer of cerebellar folium Crus IIa of freely behaving rats. *J Neurosci* 2001; 21: 3549–3563.
- Bower JM. Control of sensory data acquisition. *Int Rev Neurobiol* 1997; 41: 489–513.
- Albus JS. A theory of cerebellar function. *Math Biosci* 1971; 10: 25–61.
- Medina JF, Mauk MD. Computer simulation of cerebellar information processing. *Nat Neurosci.* 2000; 3: 1205–1211.

15. Sharp AA, O'Neil MB, Abbott LF, Marder E. Dynamic clamp: computer-generated conductances in real neurons. *J Neurophysiol* 1993; 69: 992–995.
16. Robinson HPC, Kawai N. Injection of digitally synthesized synaptic conductance transients to measure the integrative properties of neurons. *J Neurosci Methods* 1993; 49: 157–165.
17. Hanson JE, Jaeger D. Short-term plasticity shapes the response to simulated normal and parkinsonian input patterns in the globus pallidus. *J Neurosci* 2002; 22: 5164–5172.
18. Sultan F, Bower JM. Quantitative Golgi study of the rat cerebellar molecular layer interneurons using principal component analysis. *J Comp Neurol* 1998; 393: 353–373.
19. Palay SL, Chan-Palay V. *Cerebellar Cortex: Cytology and Organization*. Berlin, : Springer, 1974.
20. Llano I, Marty A, Armstrong CM, Konnerth A. Synaptic- and agonist-induced excitatory currents of Purkinje cells in rat cerebellar slices. *J Physiol (Lond)* 1991; 434: 183–213.
21. Konnerth A, Llano I, Armstrong CM. Synaptic currents in cerebellar Purkinje cells. *Proc Natl Acad Sci USA* 1990; 87: 2662–2665.
22. Vincent P, Armstrong CM, Marty A. Inhibitory synaptic currents in rat cerebellar Purkinje cells: Modulation by postsynaptic depolarizations. *J Physiol (Lond)* 1992; 456: 453–471.
23. Barbour B. Synaptic currents evoked in Purkinje cells by stimulating individual granule cells. *Neuron* 1993; 11: 759–769.
24. Isope P, Barbour B. Properties of unitary granule cell – Purkinje cell synapses in adult rat cerebellar slices. *J Neurosci* 2002; 22: 9668–9678.
25. Huang C-M, Mu H, Hsiao C-F. Identification of cell types from action potential waveforms: cerebellar granule cells. *Brain Res* 1993; 619: 313–318.
26. Vincent P, Marty A. Fluctuations of inhibitory postsynaptic currents in Purkinje cells from rat cerebellar slices. *J Physiol (Lond)* 1996; 494: 183–199.
27. Suter KJ, Jaeger D. Reliable control of spike rate and spike timing by rapid input transients in cerebellar stellate cells. *Neuroscience* 2004; 124: 305–317.
28. Williams SR, Christensen SR, Stuart GJ, Hausser M. Membrane potential bistability is controlled by the hyperpolarization-activated current  $I(H)$  in rat cerebellar Purkinje neurons in vitro. *J Physiol* 2002; 539: 469–483.
29. Jaeger D, De Schutter E, Bower JM. The role of synaptic and voltage-gated currents in the control of Purkinje cell spiking: a modeling study. *J Neurosci* 1997; 17: 91–106.
30. Jaeger D, Bower JM. Prolonged responses in rat cerebellar Purkinje cells following activation of the granule cell layer: an intracellular in vitro and in vivo investigation. *Exp Brain Res* 1994; 100: 200–214.
31. Hansel C, Linden DJ, D'Angelo E. Beyond parallel fiber LTD: the diversity of synaptic and non-synaptic plasticity in the cerebellum. *Nat Neurosci* 2001; 4: 467–475.
32. Jorntell H, Ekerot CF. Reciprocal bidirectional plasticity of parallel fiber receptive fields in cerebellar purkinje cells and their afferent interneurons. *Neuron* 2002; 34: 797–806.
33. Hiss E, Leicht R, Schmidt RF. Cutaneous receptive fields of cerebellar Purkinje cells of unanesthetized cats. *Exp Brain Res* 1977; 27: 319–333.
34. Bower JM, Woolston DC. Congruence of spatial organization of tactile projections to granule cell and Purkinje cell layers of cerebellar hemispheres of the albino rat: vertical organization of cerebellar cortex. *J Neurophysiol* 1983; 49: 745–766.
35. Woody CD, *et al.* Differences in responses to 70 dB clicks of cerebellar units with simple versus complex spike activity: (i) in medial and lateral ansiform lobes and flocculus; and (ii) before and after conditioning blink conditioned responses with clicks as conditioned stimuli. *Neuroscience* 1999; 90: 1227–1241.
36. Lisberger SG, Pavelko TA, Bronte-Stewart HM, Stone LS. Neural basis for motor learning in the vestibuloocular reflex of primates. II. Changes in the responses of horizontal gaze velocity Purkinje cells in the cerebellar flocculus and ventral paraflocculus. *J Neurophysiol* 1994; 72: 954–973.
37. Santamaria F, Jaeger D, De Schutter E, Bower JM. Modulatory effects of parallel fibers and stellate cell synaptic activity on Purkinje cell responses to ascending segment input: a modeling study. *J Comput Neurosci* 2002; 13: 217–235.
38. Destexhe A, Pare D. Impact of network activity on the integrative properties of neocortical pyramidal neurons in vivo. *J Neurophysiol* 1999; 81: 1531–1547.
39. Johnston D, Wu SMS. *Foundations of Cellular Neurophysiology*. MIT Press, 1995.
40. De Schutter E, Bower JM. An active membrane model of the cerebellar Purkinje cell I. Simulation of current clamp in slice. *J Neurophysiol* 1994a; 71: 375–400.
41. Jaeger D. Synaptic shunting of membrane currents in different neural morphologies. *Soc Neurosci Abstr* 27. Program No. 501.3.2001.